

Large Eddy Simulation of the Turbulent Flow in a Tunnel with a Localized Heat Source

This paper presents Large Eddy Simulations of a compressible turbulent flow through a duct of square cross-section with a localized heat source on its bottom wall. The potential applications are related to the accidental heat release in a road tunnel. A constant temperature T_w is imposed on all duct walls except for the spot location. Two distinct heating configurations are considered. In the first configuration, the distribution of the spot temperature is uniform and varies suddenly from T_w to $2T_w$ at the spot borders. Two additional temperature levels are also considered for this configuration: $T_h/T_w = 3$ and 4 . In the second configuration, the temperature changes linearly from T_w to $2T_w$ at the spot centre. In both cases, the Reynolds number based on bulk velocity was maintained at 6000 and the Mach number at 0.5. Numerical experiments were conducted to investigate the spatial growth of the thermal field downstream of the spot and its influence on the velocity field. It was found that the heating on the lower wall induced a clear intensification of the secondary flow with a strong reduction in size of these vortices near the heated zone. In particular, a strong impinging motion has been observed just downstream of the spot.

Cet article présente une étude numérique par simulation des grandes échelles de l'écoulement turbulent d'un fluide compressible dans un conduit rectiligne et de section droite carrée munie d'un chauffage discret appliqué sur sa paroi inférieure. A l'exception du spot de chauffage toutes les parois du conduit sont maintenues à une température constante T_w . Deux configurations de chauffage sont étudiées. Dans la première configuration la température passe directement de T_w à $2T_w$ à la bordure du spot qui est alors chauffé uniformément. Deux autres niveaux de chauffage sont aussi présentés pour cette configuration, à savoir $T_h/T_w = 3$ et 4 . Dans la deuxième configuration la température du spot varie linéairement entre son centre et sa bordure. Pour toutes les configurations le nombre de Reynolds est maintenu à 6000 et le nombre de Mach à 0.5. Les simulations numériques ont pour but d'étudier l'évolution spatiale du champ thermique et son influence sur le champ dynamique. L'étude a montré que par rapport à l'écoulement isotherme le chauffage intensifie les flux secondaires avec une nette réduction de taille dans la zone du spot de chauffage. Ce phénomène s'intensifie dans la zone en aval du spot où d'intense phénomène d'éjection verticale est observé.

A. Azzi, PhD, Eng

Laboratoire de Mécanique Appliquée, USTO
University, Oran, Algérie
Email: Abbes.Azzi@gmail.com

C. Münch, PhD, Eng

LEGI, Institut de Mécanique de Grenoble, France

S. El Alimi, PhD, Eng

Laboratoire d'Etudes des Systèmes Thermiques et Energétiques, ENIM, Tunisie

SYMBOLS

| | |
|-------|-----------------------|
| D | hydraulic diameter |
| M | Mach number |
| Nu | Nusselt number |
| Pr | Prandtl number |
| Re | Reynolds number |
| T | Temperature |
| U | velocity |
| x,y,z | Cartesian coordinates |

Greek

| | |
|--------|---------|
| ρ | Density |
|--------|---------|

Subscript

| | |
|---|------|
| w | wall |
| h | spot |
| b | bulk |

INTRODUCTION

When an accidental heat release occurs in road tunnels, the most important risk to human life is related to the effects of smoke inhalation rather than to direct exposure to heat from

fires. So, for safety assessments and emergency management, it is important to understand the behaviour of the parameters that are directly connected to the fire source and its propagation. Usually, it is important to maintain an evacuation passage that is free from smoke and hot gases. Due to the considerable progress in computational hardware, numerical experimentation became an economical way to investigate such complex heat transfer problems. As the tunnel cross-sections are generally of square or rectangular shape, it is important to use computational methods and numerical schemes that are able to capture the secondary flow occurring in such geometrical configurations. By secondary flow, we mean the flow perpendicular to the main flow direction. Previous studies (Salinaz & Métais, 2002, Hébrard et al., 2004) showed that this secondary flow called also Prandtl's flow of the second kind is relatively weak (2% of the mean streamwise velocity), but it is very relevant to the heat and momentum transport involved in the present problem. The aim of the present study is to contribute to the understanding of fire propagation in tunnels by use of large eddy simulation (LES). In the first approach, which is the subject of the present study, we use a simplified mathematical model taking into account the localized behavior of heat release. The tunnel is represented by a duct of square cross-section having its wall at constant temperature T_w . The heated spot is located at one hydraulic

diameter from the inlet and extended to one other hydraulic diameter in the streamwise direction. Its spanwise width is half the hydraulic diameter and is centered on the symmetry plane of the bottom wall. Two distinct heating configuration cases are considered. In the first one, the distribution of the spot temperature is uniform and varies suddenly from T_w to $T_h = 2T_w$ at the spot borders. This first case is referred to as Tunnel-2. In the second case, which will be called Tunnel-pr, the temperature changes linearly from T_w to $T_h = 2T_w$ at the spot centre. In both cases, the Reynolds number based on bulk velocity was maintained at 6000 and the Mach number at 0.5. Figure 1 shows a sketch of the computational domain and boundary conditions. In addition, the geometrical configuration of Tunnel-2 (uniform temperature distribution) is used to investigate the effect of heated temperature level, $T_h/T_w = 3$ and $T_h/T_w = 4$, and will be called hereafter Tunnel-3 and Tunnel-4, respectively. In all cases, the spatial growth of the thermal field downstream of the spot and its influence on the velocity field and turbulence structure are investigated.

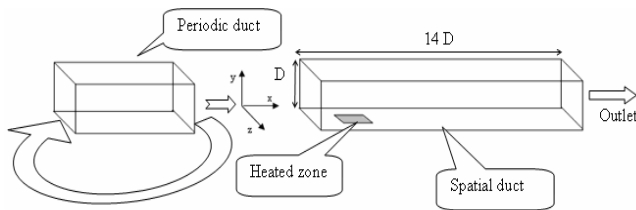


Figure 1. Computational domain and boundary conditions.

MATHEMATICAL MODEL AND NUMERICAL METHOD

The mathematical model is composed of the continuity, compressible Navier-Stokes and energy equations in the so-called fast-conservation form (Ducros et al., 1996). The equation system is non-dimensionalized by the reference dimensions: U_b - bulk velocity, ρ_b - bulk density, D - hydraulic diameter and T_w - temperature of cold walls. So, the flow parameters can be controlled by three dimensionless numbers: Re- Reynolds number, M- Mach number and Pr- Prandtl number. The system is closed by the perfect gas law where the fluid is considered as an ideal gas, the Sutherland law for molecular viscosity versus temperature and a turbulent Prandtl number fixed to 0.6. In order to reduce the computational efforts needed a low-pass spatial filter is applied to the previous governing equations. This action eliminates the scales smaller than the filter size. The effect of the sub-grid scales is taken into account by the use of an appropriate sub-grid scale model. Detailed explanation of LES formalism and numerical schemes are available in previous works (Salinaz & Métais, 2002, Hébrard et al., 2004). Only a brief description is given here. The subgrid-scale model implemented in the code is the structure function subgrid-scale model originally based on the EDQNM theory (Lesieur & Métais, 1996). Since its first version, the model is continuously improved and extensively validated in various simulations of compressible turbulent flows through isothermal and heated square ducts (Salinaz & Métais,

2002, Hébrard et al., 2004). The version used here is called the selective structure function subgrid-scale model which has a switch to activate the model only when three-dimensional turbulence occurs. The selective switch is based on the local vorticity fluctuation which is compared for each computational node to the average of their neighbours' values. The local fluid is considered to be turbulent if the direction of the two vectors is greater than a prescribed value. So, it makes the model suited to wall bounded turbulent flows without any correction. The governing equations are written in generalized coordinates and solved by extension of the fully explicit predictor-corrector McCormack scheme, second order in time and fourth order in space (Kennedy & Carpenter, 1997). The stability conditions are controlled by means of a CFL number equal to 0.5.

The size of the computational domain is set identically to previous similar computation (Salinaz & Métais, 2002) which is $14D$ times D times D (D is the hydraulic diameter) in the streamwise (x), vertical (y) and spanwise (z) directions respectively. The optimal computational grid resolution is determined as a compromise between the quality of the results and the running time. It is also set as in the same previous study (Salinaz & Métais, 2002). The 160 times 50 times 50 discretization nodes are distributed with a hyperbolic-tangent stretching law in transversal direction and uniformly distributed in the streamwise direction. The strategy for grid node distributions is to ensure a good wall resolution with 1.8 wall units perpendicular to the walls. The wall boundary conditions are set as no-slip for the velocity components and Dirichlet type for temperature. The characteristic method of Poinot & Lele (1992) is used to set the conditions at the free boundaries of the computational domain. In order to have a time-dependent solution at the inlet, an initial periodic duct is continuously resolved in such a way as to obtain a realistic inlet condition for the computational domain.

RESULTS AND DISCUSSION

In a previous numerical investigation done by Salinas and Métais (2002), a square duct with higher temperature imposed on its lower wall while the other walls are maintained at cold temperature has been considered. The main conclusion of their study is that the heated wall is subject to intense turbulence activity and the ejection mechanism from the wall is intensified by the temperature effect. It has also been reported an intensification of the secondary flows in the vicinity of the lower corners. Adjacent to vertical walls, cold air is driven from the core duct, while in the middle of the heated wall big ejections occur. Consequently, the heat flux decreases dramatically in the middle of the heated wall while it remains higher in the corners. This situation is very dangerous for industrial applications and has to be avoided. In the present case, the situation is quite different since the lower wall is heated discretely in a small region while its remaining parts are maintained at the same cold temperature as the three other walls. From a physical point of view, the fluid immediately above the heated spot forms a heated fluid zone and depending on the incoming cold fluid flow velocity, the heated fluid is convected in the longitudinal direction or not. Effectively, when an accident occurs in a road tunnel, the car traffic is immediately stopped and then the fire smoke intensifies in the vertical direction and reaches the higher tunnel wall. One solution consists of using blowers to maintain the mainstream fluid flow in order to drive the smoke outside the tunnel. So, in the presence of main fluid flow the heated fluid is convected in the mainstream direction and merges with two longitudinal counter-rotating vortices. The cold fluid is

driven from the duct core and pushed toward the bottom wall immediately downstream the heated spot.

In order to examine this phenomenon, Figure 2 presents the mean secondary flow and temperature contours in one half of duct's cross-section at the middle of the heated spot (due to the symmetry plane). When looking at Figure 2b for Tunnel-2, one can see that the sizes of the lower vortices over the heated wall are reduced and pushed toward the corners. In the heated zone and due to the heat transfer, the intensity of the ascendant fluid velocity is increased. This phenomenon disappears when looking at the corresponding case in Figure 3b, which shows the cross section at the end of the heated zone. At this location, the spanwise velocity of the lower vortices is increased and reaches 3 % of the bulk velocity versus 2 % for isothermal duct.

Figure 4a shows the instantaneous secondary flow vectors and temperature contours for Tunnel-2 at the middle of the heated spot position. As it was reported by previous investigations, the

magnitude of the instantaneous transverse flow is about ten times the corresponding mean flow field. Obviously, the scale of velocity vectors is changed in order to keep a good visibility of the figure. The temperature contours show a quasi-stationary big ejection around the middle plane. So, at the middle of the spot it is expected to have a decrease in mean wall heat flux and an increase in the turbulent activity. The Part b of Figure 4 shows that in vicinity of the hot spot, the temperature fluctuation is enhanced both in positive and negative directions. This is related essentially to the intensive turbulent activities in this region.

In order to have a good impression of the heat transfer distribution, Figure 5a shows the longitudinal distribution of the local Nusselt number along the symmetry plane while Figure 5b presents the lateral distribution of the local Nusselt number at the middle of the heated spot.

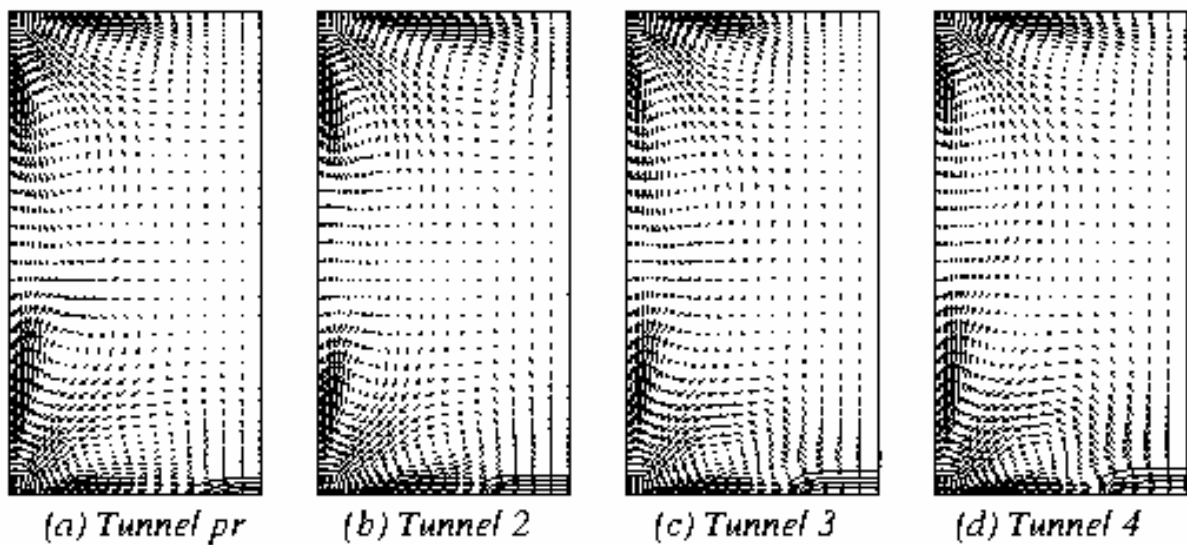


Figure 2. Mean secondary velocity vectors and isothermal contours at the middle of the hot spot.

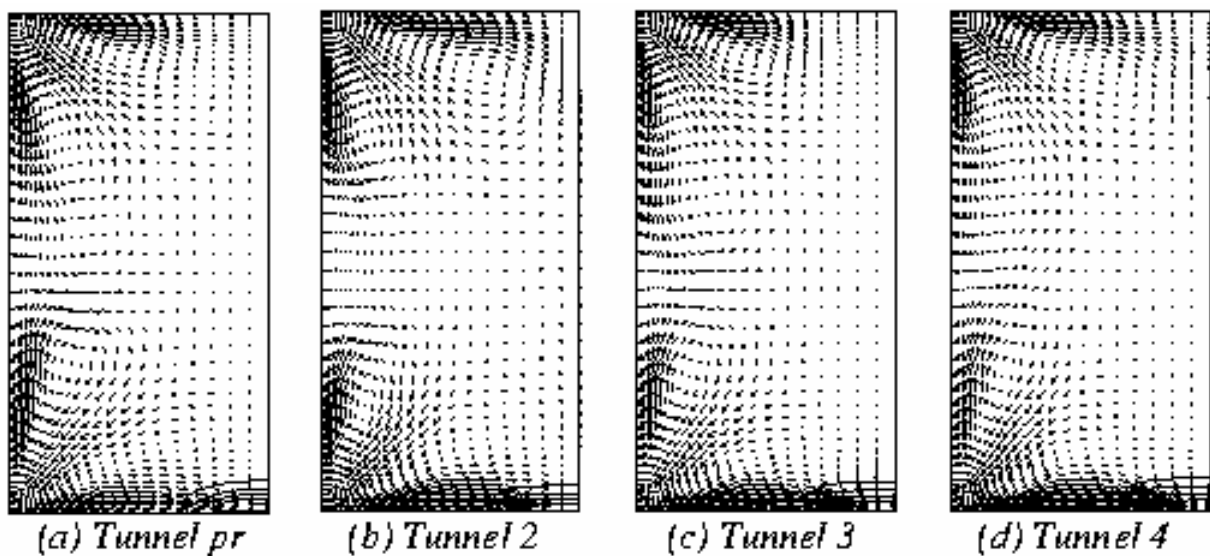


Figure 3. Mean secondary velocity vectors and isothermal contours at the end of the hot spot.

It can be seen that for all cases where the spot is uniformly heated, Tunnel-2, Tunnel-3 and Tunnel-4, the heat flux increases laterally (Figure 5b) up to its maximum on the border of the spot and then decreases in the middle of the spot according to ejection phenomena cited above. In the longitudinal direction, (Figure 5a) the wall heat flux increases in the streamwise direction. The maximum is reached at approximately the first quarter of the heated spot. Then it decreases towards the minimum value, and then increases and goes to zero ($x/D \approx 5$). As it was shown on Figure 3, downstream of the heated spot, the reinforcement of secondary flows of Prandtl's second kind brings cold fluid from the unheated walls and contributes to cooling this part of the wall. Negative Nusselt number in this region is related to the fact that the fluid temperature is higher than the maintained wall temperature T_w . Examining Figure 2 (c and d) and Figure 3

(c and d) for Tunnel-3 ($T_h/T_w = 3$) and Tunnel-4 ($T_h/T_w = 4$), respectively, the same phenomenon is reported

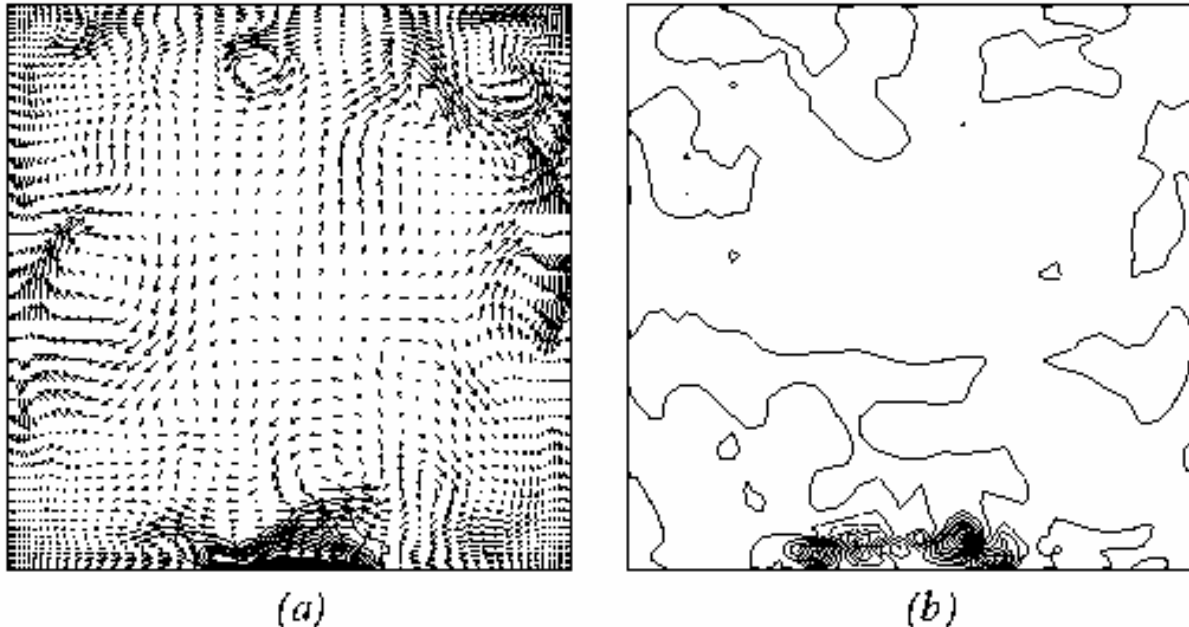


Figure 4. Cross section at the middle of the hot spot. *Tunnel-2*.
 a- Instantaneous secondary flows vectors and temperature contours
 b- Isocontours of temperature fluctuation, continue lines: positive values, dashed lines: negative values

In order to highlight some near wall turbulent structures, the contours of the longitudinal velocity fluctuations near the heated wall are plotted in Figure 6, for the two extreme cases studied, namely; Tunnel-2 and Tunnel-4. As it was noted in previous DNS and LES computations, the near wall turbulent flow structure is composed of streaks which are clearly showed in Figure 6. The dark isolines represent the low speed streaks and the grey ones represent high speed streaks. Figure 6b is related to the more heated case Tunnel-4 and shows a significant enhancement of the streak width. This is due essentially to the high temperature level, which is responsible for the viscosity augmentation. So the turbulent flow structure size is automatically increased. It was showed in a previous study [1] that the increase in the size of the injection is due to the increase in size of the streaky injection. The corresponding temperature

with more intensification. The spanwise mean secondary flow reaches 5 % for the first case and 7 % for the second one. Nevertheless, the vertical component goes to 3 % and 4 % respectively only in the positive direction. It means that only upward flow is accelerated. It seems that at this level of heating power, the higher half of the duct is not very perturbed.

According to Figure 5b, the comparison between Tunnel-pr and Tunnel-2, reveals that in the former case, where the spot is heated via a linear temperature distribution, the maximum wall heat flux is higher and slightly declined in the streamwise direction (approximately in the middle versus a quarter for the Tunnel-2 case). This is explained by the fact that in the Tunnel-pr case the maximum temperature is concentrated in a small zone at the middle of the spot. The cooled part is also slightly in advance. According to Figure 2a and 3a for Tunnel-pr, the same trends are observed but with less intensity.

fluctuation for Tunnel-4 case is represented on Figure 6c and highlights an intensive fluctuation activity in the vicinity of the heated spot.

The turbulent structures can be also represented by plotting the coherent turbulent vortices. This is shown in Figure 7a, which represents the near wall turbulent structures by means of the so-called Q criterion isolines (Hunt et al., 1988). The Q criterion is based upon the second invariant of the velocity gradient tensor and is a good tool to detect coherent vortices. As it is expected, the coherent structures are longitudinally elongated and are more concentrated around the heated zone. Figure 7b, displays the instantaneous thermal structures (isosurface $T=1.05$) and the associated secondary velocity field at two cross-sectional planes Tunnel-4. This figure shows clearly the streamwise deviation of the thermal field by the axial fluid flow.

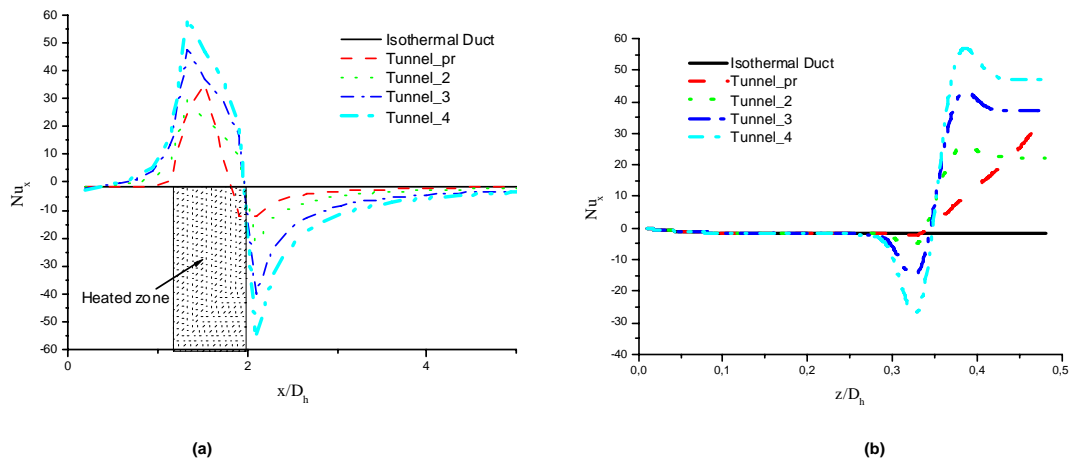
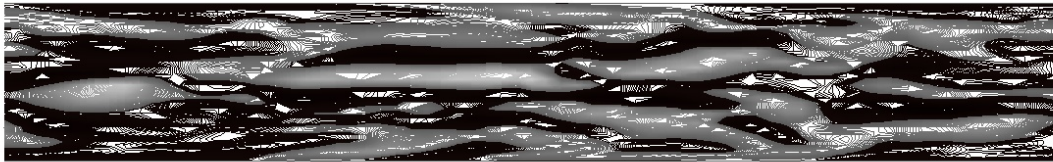


Figure 5. Local Nusselt Number distribution.

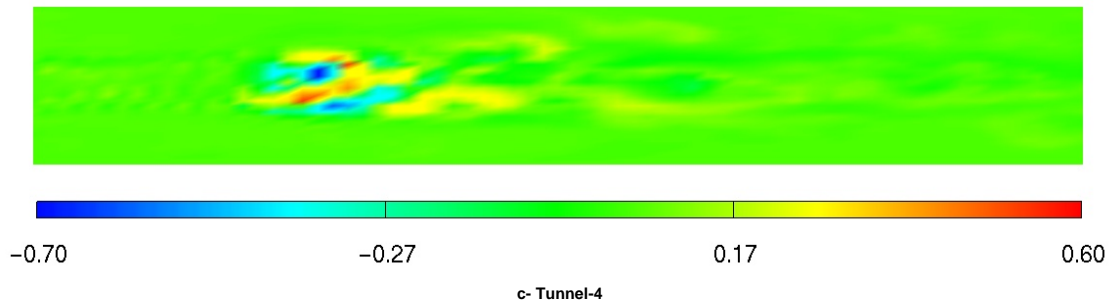
- a- Streamwise distribution of the local Nusselt Number at the symmetry plane $Z/D = 0.5$.
- b- Spanwise distribution of the local Nusselt Number at the middle of the hot spot.



a- Tunnel-2



b- Tunnel-4



c- Tunnel-4

Figure 6. Isolines of fluctuating streamwise velocity near the heated wall, plan x,z at $y+=15$. Dark isolines represent low speed streaks ($-0.5 < u < 0$) and grey isolines represent high speed streaks ($0 < u < 0.5$). a- Tunnel-2, b- Tunnel-4, c- Isolines of temperature fluctuations, Tunnel-4

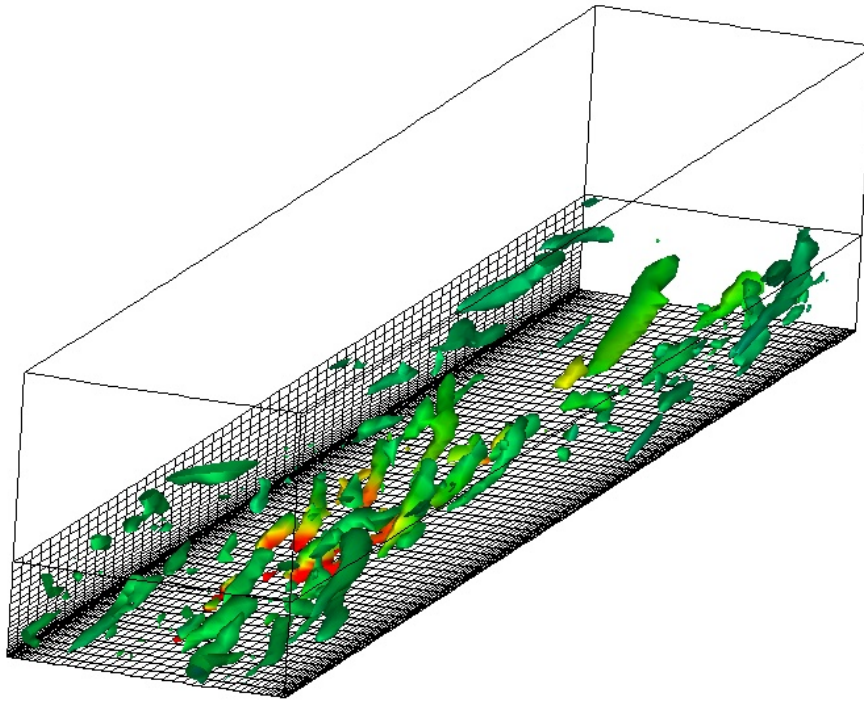


Figure 7a. Tunnel-4, Coherent turbulent structures shown through the Q criterion, $Q=0.6$

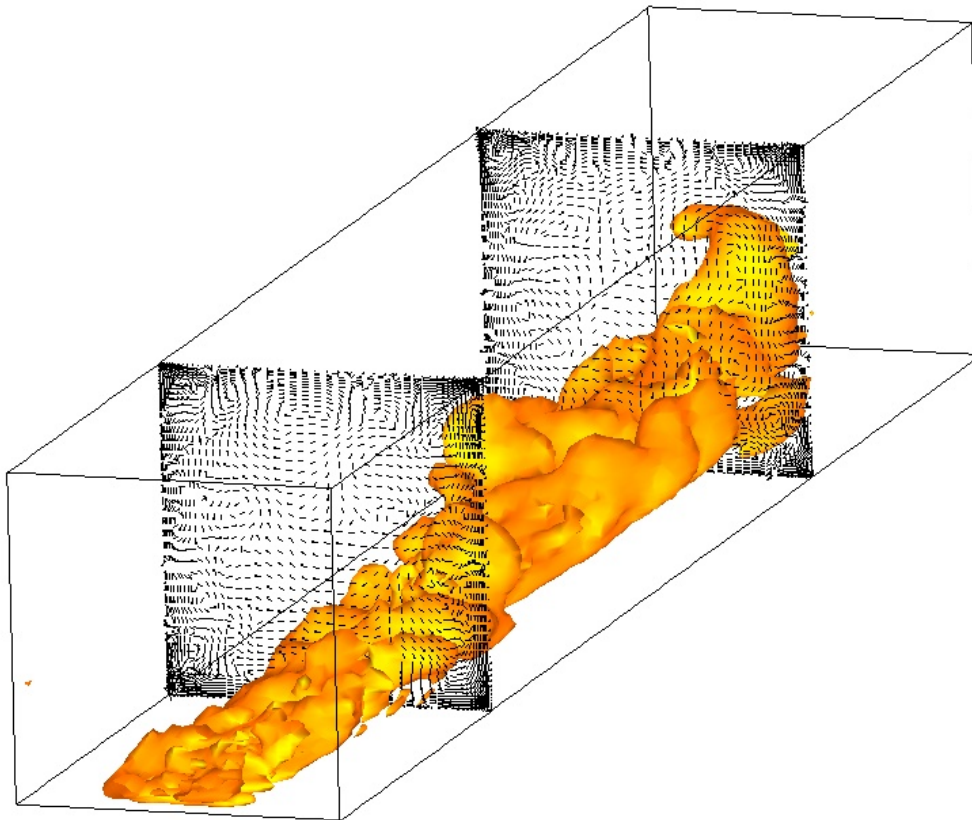


Figure 7b. Tunnel-4, Isosurface of instantaneous temperature $T=1.05$ and instantaneous secondary velocity field at two cross-sectional planes

CONCLUSIONS

In the present paper, the effect of a localized heat source on the bottom wall of a duct with square cross-section is investigated through the large-eddy simulation technique. This study focuses on secondary flow and thermal field modifications with respect to the hot temperature level and its distribution. It was found that the secondary flows near the heated zone are enhanced in intensity. In the vicinity of the heated zone, the viscosity is increased due to the heating effect. So, the coherent turbulent structures are enhanced in size and are responsible for strong ejection phenomena in the middle of the heated spot. We are presently developing a more advanced mathematical model taking into account the gravity effect to realistically reproduce fire dynamics for tunnel applications.

ACKNOWLEDGMENTS

Financial support was provided by the CETU (Centre d'Etudes des Tunnels, Nice France) and AUF (Agence Universitaire de la Francophonie).

REFERENCES

1. Salinas-Vazquez, M. & Métais, O., 2002, Large-eddy simulation of the turbulent flow through a heated square duct. *J. Fluid Mech.*, 453, pp. 201-238.
2. Hébrard, J., Métais, O. & Salinas Vazquez, M., 2004, Large-eddy simulation of turbulent duct flow: heating and curvature effects, *Int. Journal of Heat and Fluid Flow*, pp. 569-580.
3. Ducros, F., Comte, P. & Lesieur, M., (1996) Large-eddy simulation of transition to turbulence in a boundary-layer developing spatially over a flat plate, *J. Fluid Mech.* 326,1-36.
4. Lesieur, M. & Métais, O., (1996) New trends in large eddy simulations of turbulence, *Annu. Rev. Fluid Mech.* 45-82.
5. Kennedy, C. A., Carpenter, M. H. (1997) NASA technical paper Paper 3484.
6. Poinsot, T. & Lele, S., (1992) Boundary conditions for direct simulations of compressible viscous flows, *J. Computational Physics*, 104-129.
7. Hunt, J., Wray, A. & Moin, P. (1988) Eddies, stream, and convergence zones in turbulent flows, Centre for turbulence Research Rep. CTR-S88.